applied sciences

MDPI

Article

Numerical Investigation of the Slope Stability in the Waste Dumps of Romanian Lignite Open-Pit Mines Using the Shear Strength Reduction Method

Florin Dumitru Popescu [1,*], Andrei Andras [1,*], Sorin Mihai Radu [1], Ildiko Brinas [1] and Corina-Maria Iladie [2]

[1] Department of Mechanical, Industrial and Transport Engineering (IMIT), University of Petroșani, 332006 Petroșani, Romania; sorin_mihai_radu@yahoo.com (S.M.R.); kerteszildiko@ymail.com (I.B.)
[2] Doctoral School in Mines, Oil and Gases, University of Petrosani, 332006 Petrosani, Romania; iladie.corina@yahoo.com
* Correspondence: fpopescu@gmail.com (F.D.P.); andrei.andras@gmail.com (A.A.)

Abstract: Open-pit mining generates significant amounts of waste material, leading to the formation of large waste dumps that pose environmental risks such as land degradation and potential slope failures. The paper presents a stability analysis of waste dump slopes in open-pit mining, focusing on the Motru coalfield in Romania. To assess the stability of these dumps, the study employs the Shear Strength Reduction Method (SSRM) implemented in the COMSOL Multiphysics version 6 software, considering both associative and non-associative plasticity models. (1) Various slope angles were analyzed, and the Factor of Safety (FoS) was calculated, showing that the FoS decreases as the slope angle increases. (2) The study also demonstrates that the use of non-associative plasticity leads to lower FoS values compared to associative plasticity. (3) The results are visualized through 2D and 3D models, highlighting failure surfaces and displacement patterns, which offer insight into the rock mass behavior prior to failure. (4) The research also emphasizes the effectiveness of numerical modeling in geotechnical assessments of stability. (5) The results suggest that a non-associative flow rule should be adopted for slope stability analysis. (7) Quantitative results are obtained, with small variations compared to those obtained by LEM. (6) Dilatation angle, soil moduli, or domain changes cause differences of just a few percent and are not critical for the use of the SSRM in engineering.

Keywords: mine waste dump; slope stability; shear strength reduction method; Comsol; factor of safety (FoS)

Citation: Popescu, F.D.; Andras, A.; Radu, S.M.; Brinas, I.; Iladie, C.-M. Numerical Investigation of the Slope Stability in the Waste Dumps of Romanian Lignite Open-Pit Mines Using the Shear Strength Reduction Method. *Appl. Sci.* **2024**, *14*, 9875. https://doi.org/10.3390/app14219875

Academic Editors: Tongchun Li and Chaoning Lin

Received: 2 October 2024
Revised: 18 October 2024
Accepted: 23 October 2024
Published: 29 October 2024

1. Introduction

Open-pit mining is one of the surface mining methods usually employed to extract near-surface deposits of ores, nonmetallic minerals, or fossil fuels from the earth's surface. It often results in a high productivity and requires large capital investments, low operating costs, and good safety conditions [1–3]. Due to growing open-pit mining activities, their effect on the environment has also increased [4–6]. The impacts of open-pit mining and mineral processing plants on the environment are diverse, as presented by Dudka et al. [7] and Firozjaei et al. [8] in their reviews, and include land degradation, as studied by Tran et al. [9,10] in their works; noise, dust, and poisonous gasses released during mining and processing, as evaluated by Saini et al. [11] in India and Popović et al. [12] in Serbia and Romania, who concluded that the most severe impact in these countries is caused by dust and greenhouse gasses above safety limits; and the pollution of water which was thoroughly analyzed for the mining industry in China by Li et al. [13].

As a direct result of the processes that occur during open pit mining, significant amounts of waste material are generated, which are transported to and accumulated in deposits referred to as overburden or waste dumps, which are usually constructed near the

mining site [14,15]. These waste dumps pose a multitude of challenges, including the degradation of soil fertility, the loss of biodiversity, and the potential pollution of the surrounding environment through the leaching or escape of sulfide and other toxic substances.

The sheer scale and volume of these waste dumps have increased in recent years, leading to the construction of ever-higher dump structures to minimize the ground cover area. This increase in height has heightened the risk of slope failures, which can have catastrophic consequences [16–18] potentially leading to the collapse of the dump structures, triggering landslides or debris flows that could jeopardize the personal and property safety of mining personnel and nearby residents.

The inherent instability of mine waste dumps, due to their loose structure and high water content, has prompted scholars in open-pit mining to recognize the importance of analyzing waste dump stability. The term used to describe the safety margin of slopes in waste dumps and other geotechnical structures is the "Factor of Safety", abbreviated as FoS. In general engineering, the FoS represents the margin by which a system exceeds the strength required to support its intended load. In particular, in geotechnical engineering, the FoS is a ratio which compares the shear strength (forces resisting movement) of a slope against the shear stress (forces driving the slope towards failure). An FoS greater than 1 indicates stability of the slope as the resisting forces exceed the driving forces, while an FoS less than 1 indicates instability of the slope and its failure. More recent research indicated that the safe value of the FoS should be above the 1.45–1.50 limit. In practical terms, the FoS provides an indication of how near a slope is to failure, acting as a crucial benchmark in evaluating slope stability. Consequently, evaluating the stability of waste dumps has become a critical component of mine operations [19–22]. Yang et al. [23] and Xu et al. [24] summarize several ways that can be used to assess the stability of these geo-structures. According to Masoudian et al. [25] and Popescu et al. [26], the assessment techniques either use the classic theories in limit equilibrium analyses (LEAs) [27–31] and variations of these [32–34], or probabilistic analyses (PA) [35–39] or numerical modeling analyses (NMA) [40–46]. According to Xu et al. [47], in recent years, the development of machine learning (ML) has allowed for it to be extensively used in stochastic slope stability analysis, particularly to improve computational efficiency. Nevertheless, the majority of these studies do not consider the combined impact of slope geometry and non-associative plasticity models, which the present study explores.

LEA methods evolved from the analytical ones developed in 1930s towards their implementation in computer software that is able to compute both the Factor of Safety (FoS) and the location of the critical slip surface more quickly and accurately.

In contrast to LEA, PA allows for the uncertainty of input variables to be quantified and incorporated into the analysis, so besides an approximate value of the FoS, an approximate value of the failure probability is also obtained. PA should not be viewed as a substitute for the classic deterministic methods, but as a complementary approach.

Several existing ML methods that have been used for slope stability analyses in the last decade were reviewed in [48]. Out of these, artificial neural networks [49] are the most common, with Support Vector Machine [50] and various Regression Algorithms [51] also being extensively used.

Finally, NMA can simulate the behavior of complex, real-life geotechnical problems using software code, and provides the most accurate values for the FoS. The computational power available today allows multiple parameters to be taken into account, like internal friction angles, material cohesion, slope height, slope angle, pore water pressure, and the unit weight of rock and soil, etc. NMA can employ continuum numerical modeling techniques, such as the finite element method (FEM), finite difference (FD), and the boundary element method (BEM); discontinuum modeling, such as the discrete elements method (DEM) and the universal distinct element code (UDEC); and coupled continuum and discontinuum modeling for very complex conditions, including the combined finite-discrete element method (FDEM). The DEM was introduced [52] as a discontinuum-based method that is capable of modeling and simulating the failure of discontinuous media such as jointed

rock slopes [53,54], and can be coupled successfully with the Shear Strength Reduction Method [55].

In their comprehensive review [56], Gupta et al. emphasize that the SSRM is adopted in the majority of studies that use FEM, DEM, or FD to analyze waste dump slope stability.

For the current study, SSRM was chosen for its ability to handle non-linear material behavior more effectively compared to LEA, which is especially important in the case of mine waste dumps, considering their heterogenous and loose structure. Several scientists like Griffiths et al. [57], Dyson et al. [58], and Sun et al. [59] presented several advantages of this method over traditional ones, concluding that in the case of the SSRM when failure occurs 'naturally', the location of the critical failure surface is obtained without the need for a trial and error or the limitations of the interslice shears as in LEA, and it can consider complex factors that affect slope stability.

The SSRM was proposed initially by Zienkiewicz et al. [60] and involves progressively reducing the shear strength of the material in small increments, to bring the slope to the state of limit equilibrium (failure). The series of iterations are carried out using trial values of the strength reduction factor in order to reduce the values of cohesion and the internal angle of friction, until either the slope failure occurs or a limiting condition is obtained following the Mohr–Coulomb failure criterion. Since its initial use, various developments and variations of the method have been proposed. Scholars like Griffiths [61], Naylor [62], Smith et al. [63], and Matsui et al. [64] made the first improvements in the early 90s. More recently, Zhu et al. [65] modified and used the SSRM to prove its feasibility for the evaluation of locally loaded slopes, by combining the numerical method with physical studies. The safety and stability of an open-pit mine waste dump from Tibet was assessed by Zou et al. [66], using a novel combination of in-site measurements and numeric simulations performed in MIDAS and FLAC codes, with each analytical step being calculated through the SSRM. The SSRM was further enhanced by incorporating a hierarchical multiscale approach developed by Meng et al. [67], who introduced micromechanical parameters such as normal cohesion, tensile cohesion, and the angle of friction, to establish a new computational tool for heterogeneous geomaterial slope stability analysis. An improved numerical manifold method [68] with multiple layers of mathematical cover systems [69] was proposed by Yang et al., to analyze the stability of the soil–rock mixed slopes, by modifying Young's modulus and Poisson's ratio during the factor of safety (FoS) calculation using the SRM technique. This year, a technique called root bracketing was used by Dyson et al. [70] to enhance the SSRM's efficiency when performing slope stability analysis, allowing the minimization of the number iterations that need to be computed in order to determine the FoS.

Several software products such as FLAC3D and 3DEC [71,72], Plaxis3D [73,74], Phase2 and Slide [75,76], or Comsol Multiphysics [77] use SSRM to compute the FoS for slopes of various geotechnical constructions such as dams, embankments, and waste dumps. Each software has its own strengths and weaknesses, so the choice of a particular software is based on the particularity of the problem that needs to be solved and the experience of the user.

COMSOL is used by Wu et al. [78] to determine the stability of a slope considering a coupled model subjected to thermal (temperature variation), hydraulic (water pressure), and mechanical (stress/displacement) processes, with the results being validated by three experimental and numerical case studies. In their study [79], Shao et al. again used COMSOL to solve a coupled slope stability and hydrological model, for both single- and dual-permeability flows. The results obtained by the simulation were compared against two examples in order to validate the findings. An optimized version of the SSRM is proposed by Sysala et al. [80] to compute an embankment stability problem considering unconfined seepage. Matlab code was used to optimize the solution obtained using various Davis' approaches and the results were compared with the commercial Plaxis and COMSOL Multiphysics software's results. Another study conducted by Sysala et al. [81] validates the FoS obtained by an optimized variant of the shear strength reduction method in the case of three embankments with unconfined seepage, and they propose a comparison using

Plaxis and COMSOL between SSRM, modified SSRM, and optimized MSSRM on numerical examples representing a case study of a real heterogeneous slope. The stability analysis of rocks surrounding a natural underground natural gas storage has been performed by Zhang et al. [82] using the capabilities of COMSOL and Matlab, taking into consideration the effect of mechanical stress and low temperature.

Based on its use for solving various stability problems as presented above, and considering the past experiences [83,84] of the authorial team in using it, COMSOL Multiphysics software was chosen for the present study.

The aim of this study is to evaluate the stability of waste dumps using different slope angles under both associative and non-associative plasticity models. To achieve this, a series of steps were taken: (i) A model was constructed based on real waste dumps from two lignite exploitations situated in the Motru coalfield, located in the Oltenia region of Romania. (ii) For that model, a stability analysis was conducted for various slope angles, considering geometric dimensions compatible to the real slopes, and geotechnical characteristics of the material from those waste dumps. (iii) FoS values were determined for the angles considered using the commercial software COMSOL Multiphysics, based on the shear strength reduction method implemented using the software, and (iv) for each angle, both non-associative and associative plasticity was considered for the material. The obtained results were close to the expected ones, based on past calculations recorded by the mining company and research conducted at their request.

2. General and Theoretical Aspects Regarding Slope Stability

A slope represents a flat surface inclined at a certain angle α relative to the horizontal, ensuring the connection between two different elevations and bordering an earth mass. The design of slopes involves determining their optimal inclination to ensure the stability of the earth mass. Too steep slope angles may lead to instability, while overly gentle slopes represent uneconomical solutions (requiring large volumes of excavation and occupying significant land areas).

The classical methods used in geotechnical practice for analyzing the general stability of sloped earth masses evaluate the static equilibrium of an earth mass, which is limited at the bottom by a slip surface and at the top by the ground surface. This earth mass tends to move under the influence of gravitational forces. Plane sections are analyzed, and the conditions of a plane strain state are considered.

More recently, the method of strength reduction combined with the finite element method has been increasingly applied to solve geotechnical slope stability problems. This method proves to be a useful tool for determining the factor of safety (FoS), which can be applied to evaluating the stability of slopes, natural hillsides, specific embankment slopes, open-pit steps, and waste dumps.

Besides the slope's geometry, stability is influenced by the physical and mechanical characteristics of the material (soil or rock) making up the earth mass. In the strength reduction method, the material's characteristic properties are progressively reduced until failure occurs.

The FoS is considered to be an indicator of stability, which, in the context of geotechnical problems, is defined as the ratio between the limit (failure) value of the material's strength parameter (typically shear stress) and its actual value under given geometric and loading conditions.

The strength reduction method is applicable primarily to linear failure criteria such as the Mohr–Coulomb criterion. When using the Mohr–Coulomb criterion with this method, the values of cohesion, the internal friction angle, and the dilatation angle are reduced simultaneously until mechanical equilibrium is lost.

As the material parameters decrease, the soil's shear strength reduces, eventually leading to slope instability. This phenomenon causes the slope to slide under a specific combination of loads, material properties, and boundary conditions. The ratio between the initial cohesion and the cohesion at failure determines the FoS.

The COMSOL software package is suitable for solving slope stability problems as it includes modules for implementing models in terms of geometry, material properties, failure (yielding) assumptions, and the necessary computational algorithms for applying the strength reduction method.

The material properties for applying the Mohr–Coulomb model are expressed in relation to the FoS. Thus, in a parametric study the soil's strength characteristics are reduced by gradually increasing the FoS with each iteration step. The actual FoS is reached when the model no longer converges, signifying the point at which slope failure (sliding) occurs.

The yield function F and plastic potential Q for the Mohr–Coulomb failure hypothesis are given by the relations:

$$F = m\sqrt{J_2} + \frac{\sin\Phi}{3} I_1 - C\cos\Phi \tag{1}$$

$$Q = m_q\sqrt{J_2} + \frac{\sin\Psi}{3} I_1 - C\cos\Psi \tag{2}$$

where I_1 and J_2 are the first and second invariants of stress.

The parametrized material properties (Φ—parametrized internal friction angle; C—parametrized cohesion; and Ψ—parameterized angle of dilatation) are expressed as:

$$C = \frac{c}{\mathrm{FoS}},\ \Phi = \arctan\left(\frac{\tan\phi}{\mathrm{FoS}}\right),\ \Psi = \left(\frac{\tan\Psi}{\mathrm{FoS}}\right) \tag{3}$$

where c is the cohesion, ϕ is the internal friction angle, and ψ is the angle of dilatation; these are the unreduced initial parameters of the material.

In the case of the associative flow rule, the condition ψ = ϕ has to be met. For the non-associative flow rule, the angle of dilatation ψ remains constant as long as it is smaller than the internal friction angle Φ [85]. For our study, the angle of dilatation was considered null when applying the non-associative flow rule, meaning no special adjustments are necessary and (3) can be used for both the associative and non-associative flow rules.

It must be noted that, when the non-associative flow rule is used, the strength reduction method may produce numerical instabilities, leading to non-unique values for FoS and failure. In order to prevent these convergence problems, refs. [86] suggested the use of reduced strength parameters as initially proposed in [87] as the Davis Procedure B. This involves using the associative flow rule, but with values for the internal friction angle and the cohesion reduced, in order to simulate the effects of the non-associative flow rule. The reduced internal friction angle ϕ′ and reduced cohesion c' are calculated using:

$$c' = \beta c,\ \phi' = \arctan(\beta \cdot \tan\phi) \tag{4}$$

where β is the strength reduction factor that can be expressed as:

$$\beta = \frac{\cos\left(\arctan\left(\frac{\tan\phi}{\mathrm{FoS}}\right)\right)\cos\left(\arctan\left(\frac{\tan\Psi}{\mathrm{FoS}}\right)\right)}{1 - \sin\left(\arctan\left(\frac{\tan\phi}{\mathrm{FoS}}\right)\right)\sin\left(\arctan\left(\frac{\tan\Psi}{\mathrm{FoS}}\right)\right)} \tag{5}$$

As a result, (3) is rewritten considering the reduced cohesion c' and the reduced internal friction angle ϕ′ for both the associative and non-associative flow rules, because the reduction factor β = 1 in the associative flow rule.

3. Description of Location and Geometry of the Model

Incidents caused by stability issues in waste dumps in the Oltenia coal mining region (Figure 1), manifested as landslides involving large volumes of waste material, amounting to millions of cubic meters and impacting both the natural and built environments, have been recorded at several external dumps at various open-pit mines.

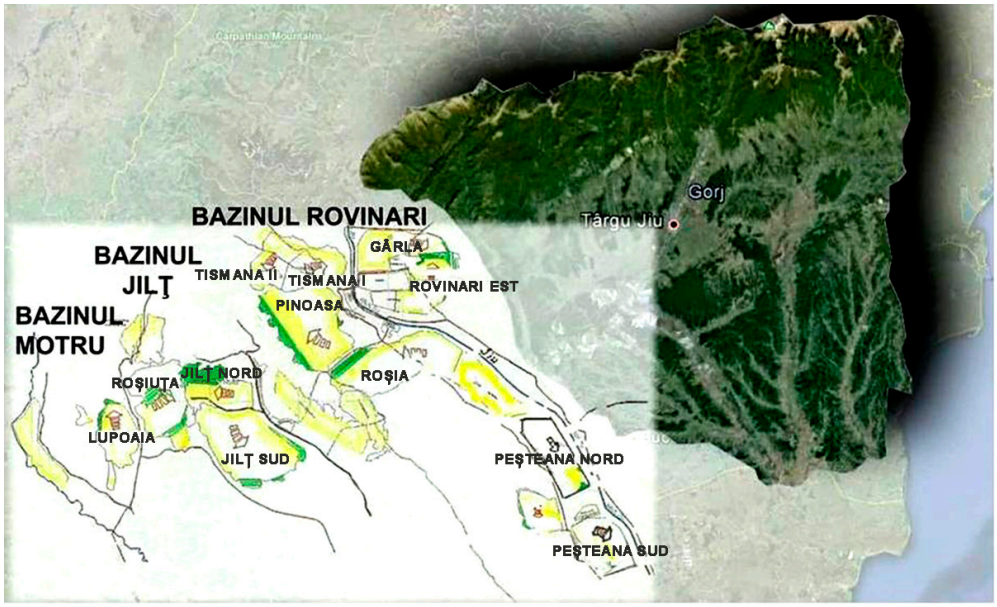

Figure 1. Basins in the Oltenia coal mining region [Oltenia Energy Company internal documents].

The issue of dump stability is not limited to the construction period during which the waste material is deposited and leveling and sloping works are carried out. As evidenced by the aforementioned incidents, the stability problem extends over a considerable period after the dumping activities have ceased.

This necessitates the monitoring of movements in unstable areas within the exploitation perimeter, its surroundings, and the dumps themselves should be conducted both during the exploitation period and for a sufficiently long period after the cessation of dumping activities.

To illustrate the method, we adopted a model that is morphologically and dimensionally compatible with most of the dumps in the Motru coal basin. Figure 2 shows the cross-section of the sloped mass model. The lengths L_1 and L_2 are 85 m and 20 m, respectively, while the heights H_1 and H_2 are 20 m and 10 m, respectively. The slope angle α varies from 30° to 45°, which corresponds to the range of both designed and real slope angles for most dumps in the Motru coal basin.

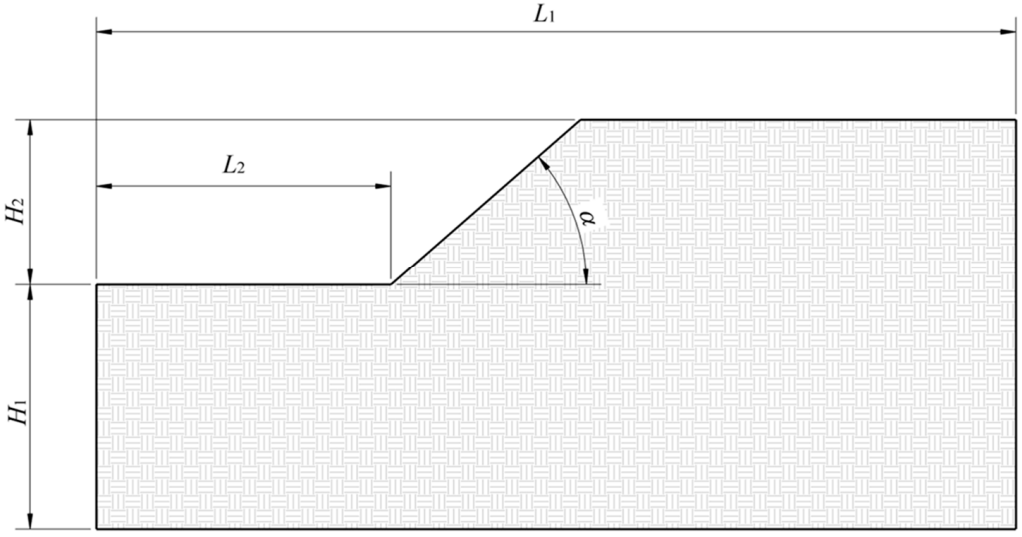

Figure 2. Cross-Section of the rock mass model.

The material properties for both non-associative plasticity—noted as Material 1—and associative plasticity—noted as Material 2—are summarized in Table 1. The values are the mean (average) values for the soil properties of the material dumped in the waste deposits from the analyzed Lupoaia and Roșiuța exploitations in the Motru coal basin and are based on a real data series that the Oltenia Energy Complex has in its records [88,89], as determined during the mandatory periodic laboratory testing of soil samples [90]. In the modeling, the plane strain assumption is applied for the sloped mass in the cross-section (2D), and the calculations are performed taking into consideration the effects of gravitational acceleration.

Table 1. Material properties for the model.

Material Property	Symbol	Non-Associative Plasticity (Material 1)	Associative Plasticity (Material 2)
Young modulus	E	25 MPa	25 MPa
Poisson's ratio	ν	0.35	0.35
Cohesion	C	18 kPa	18 kPa
Angle of friction	φ	30°	30°
Angle of dilatation	ψ	0°	30°
Density	ρ	1900 kg/m^3	1900 kg/m^3

A sensitivity analysis is usually carried out by changing parameter values one at a time and checking how this affects a certain system. In order to verify our model, the sensitivity analysis was conducted by running one simulation with the same angles and flow rules, but with a change in the angle of dilatation ψ to a value of 15°, which represents 50% of the maximum value of 30° used in the main simulation. The resulting FoS value and its variation are presented in Table 2. The change noted Δ in FoS is between 0.95% and 1.96%, which means that the change in the angle of dilatation does not influence the result to a large degree, hence the model can be considered well calibrated and valid.

Table 2. FoS values and percentage change compared to angle of dilatation of 30°.

Result	Unit	Associative Flow Rule with ψ = 15°			
		A = 30°	A = 35°	A = 40°	A = 45°
FOS	1	2.09	1.86	1.68	1.53
Δ (compared to ψ = 30°)	%	0.95	1.61	1.78	1.96

The simulations were performed in COMSOL Multiphysics using a 2D model and the `Structural Mechanics` -> `Solid Mechanics` module, and using the values defined in Table. 1 for the material parameters for both considered scenarios—associative plasticity and non-associative plasticity. The difference between the two scenarios is given as the value of the dilatation angle parameter, which is 0 and 30 degrees, respectively.

Next, in the `Definiton` menu of the software, the calculation formulas corresponding to the variables (parametrized and reduced cohesion and friction angle, and the reduction factor) used in the simulation were implemented.

The general geometry of the model was constructed using `Polygon` type graphic primitives, which were later unified using the `Form Union` option. In the model construction, the region for geometry redefinition with finite elements (`Mesh Control Domains`) was also defined, as shown in Figure 3.

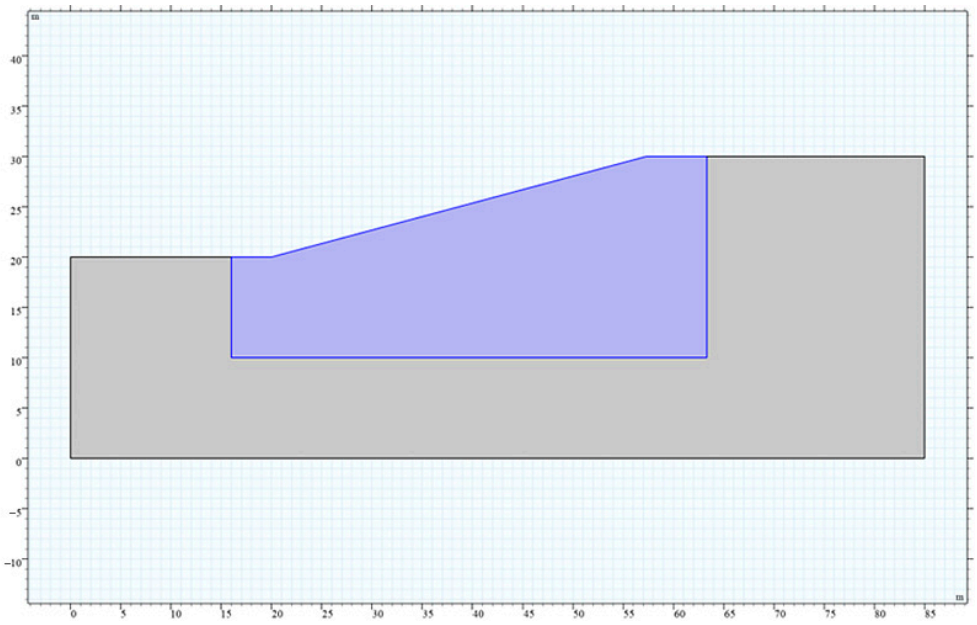

Figure 3. General geometry construction and redefinition region of finite elements model.

In the `Solid Mechanics` section, the `Quartic Lagrange` option was to define the displacement field. Also, in this section, for `Soil Plasticity`, the `Mohr-Coulomb` option was chosen for the yield criterion, and the `Associated` option was selected for the plastic potential. Regarding the initial values of stress and strain, two studies were used. The initial study evaluates the in situ stresses due to gravity, and a second study uses the results of the first study as the initial stress values. The value of the gravitational acceleration that acts on the entire domain subjected to the simulation was assigned as a Comsol constant in the simulation `--g_const`.

The domain boundaries with vertical sliding displacement (Roller) were defined, as shown in Figure 4a where these boundaries are highlighted in blue. The fixed boundaries of the domain are also highlighted in blue, as shown in Figure 4b. The free boundaries of the domain are illustrated in Figure 4c. The corresponding variables for the material properties as defined in the simulation are presented in Table 3.

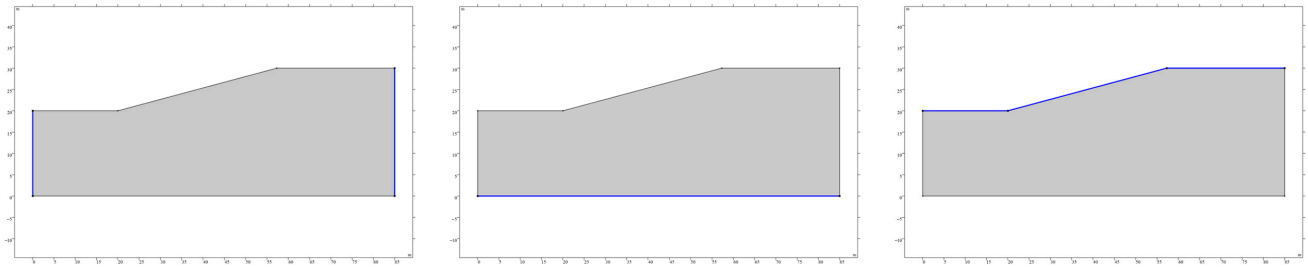

(**a**) (**b**) (**c**)

Figure 4. Boundaries of the simulation domain: (**a**) vertical sliding displacement; (**b**) fixed; (**c**) free.

Table 3. Variables corresponding to material properties defined in the simulation.

Property	Variable	Value	Unit	Group
Young modulus	E	`E_soil`	Pa	Base
Poisson's ratio	ν	`nu_soil`	1	Base
Density	ρ	`rho_soil`	kg/m^3	Base
Cohesion	C	`c_p`	Pa	Mohr-Coulomb
Angle of friction	φ	`phi_p`	rad	Mohr-Coulomb

The finite element geometry of the model is shown in Figure 5. For the entire domain under simulation, the `Finer` option was chosen for the element size, while the `Extremely Fine` option was selected for the redefinition region. The geometric shape of the finite elements is triangular.

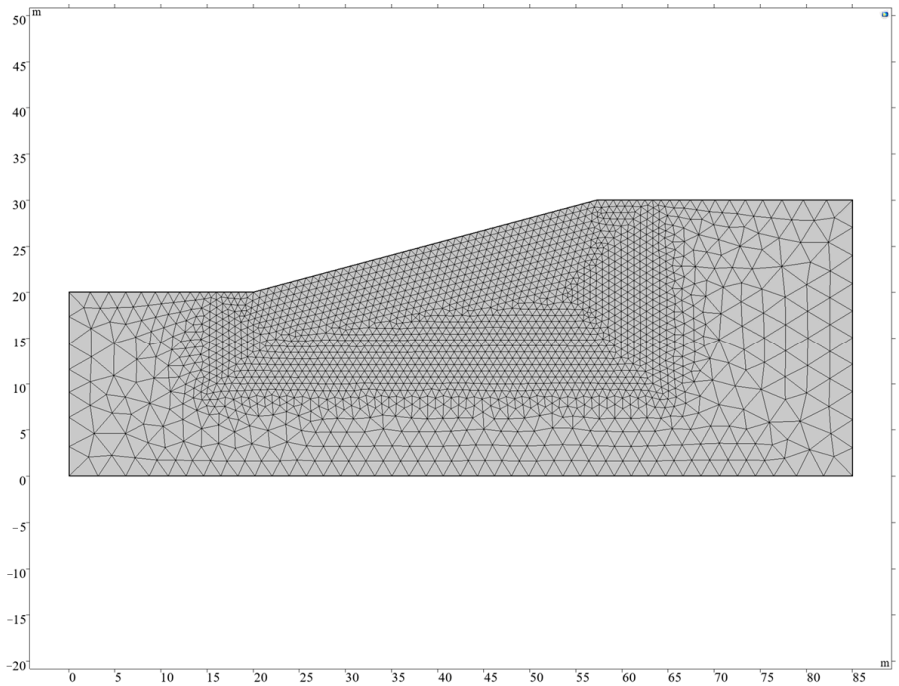

Figure 5. The finite element mesh of the model.

4. Simulation Results and Discussion

The simulation was run and the Factor of Safety (FoS) was determined for four different slope angles of 30°, 35°, 40°, and 45°. We found that the FoS decreases as the slope angle increases, which was expected, and additionally, the FoS for a similar slope angle is lower for Material 1—non-associative plasticity—compared to Material 2—associative plasticity). These results are graphically shown in Figure 6, and are consistent with those reported in [77,78].

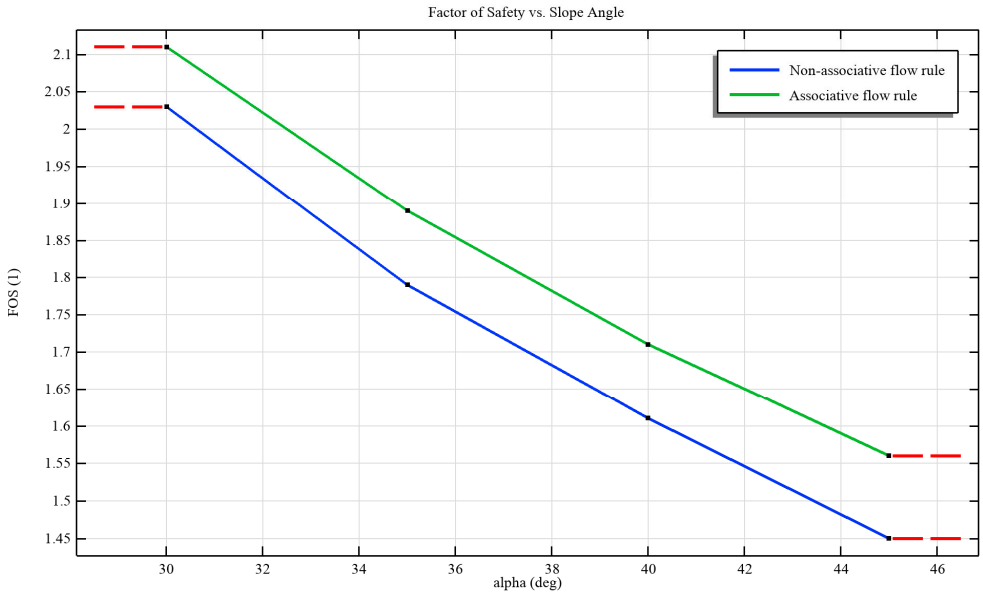

Figure 6. FoS as a function of the slope angle.

The equivalent plastic strain for all of the different slope angles, just before failure, is shown in Figures 7 and 8 for the two considered materials. The localization of the plastic strain nuclei in these figures provides an indication of the failure surfaces for the different slope angles. For smaller slope angles, multiple failure surfaces develop within the rock mass.

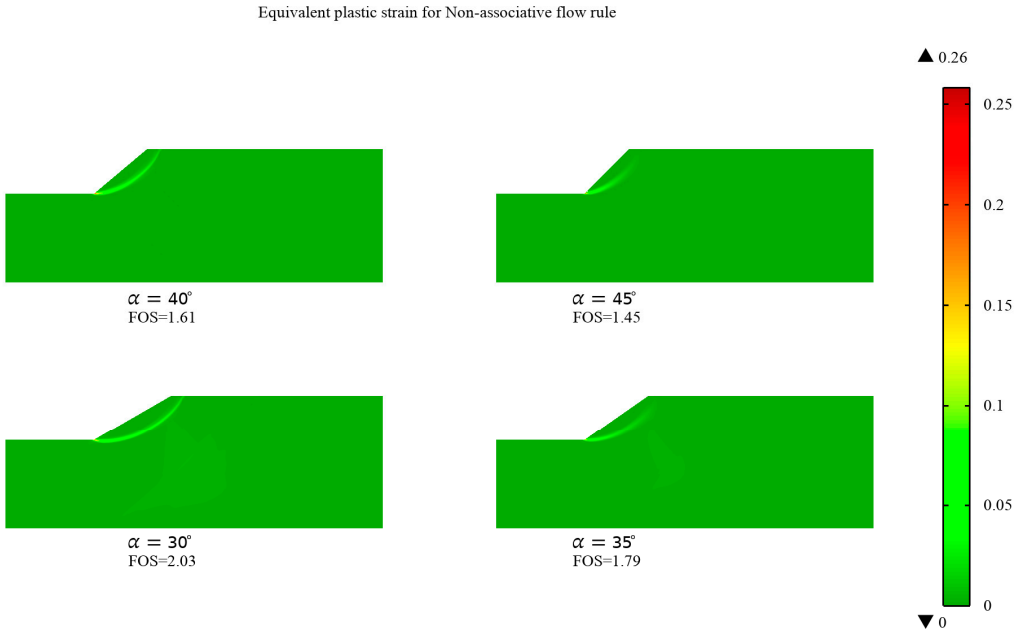

Figure 7. Equivalent plastic strain as a function of slope angle, Material 1.

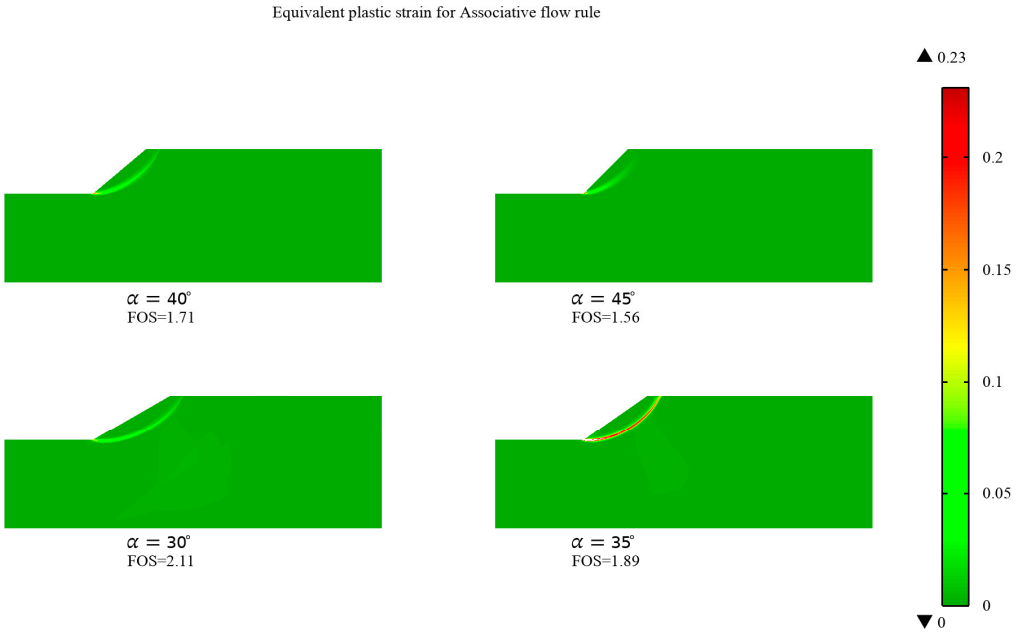

Figure 8. Equivalent plastic strain as a function of slope angle, Material 2.

A 3D visualization of the displacement is shown for a slope angle of 45° for both material types in Figures 9 and 10. This slope angle was chosen for the tridimensional presentation as it has the lowest corresponding FoS of 1.45 for the non-associative flow rule and 1.56 for the associative flow rule. The qualitative results are supported by previous research conducted using LEM [91–93]. The obtained values also show how parts of the sloped rock mass outside the slip surface begin to slide once the material becomes unstable.

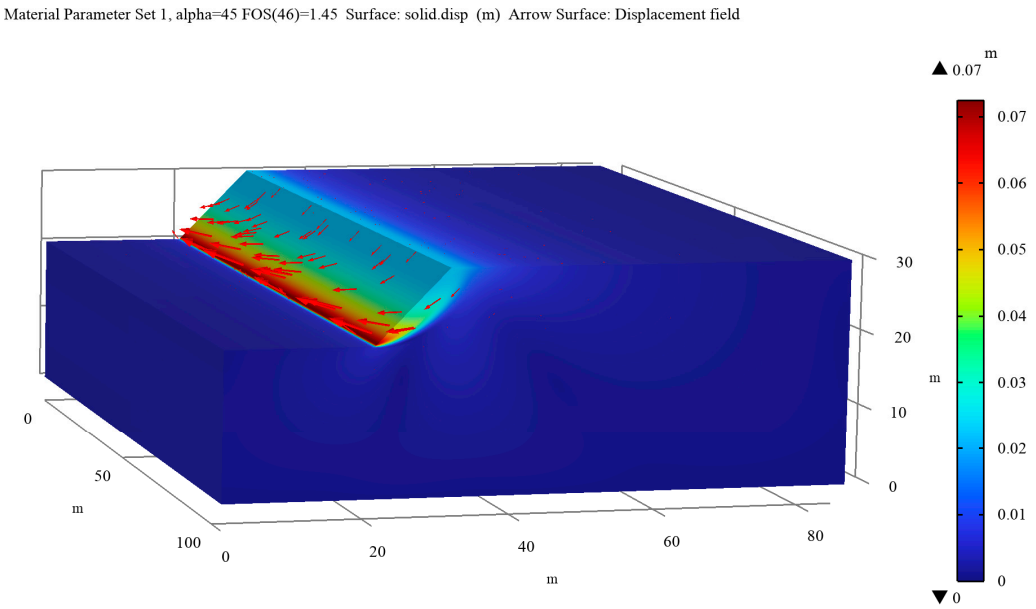

Figure 9. Displacement magnitude for a slope angle of 45°, Material 1.

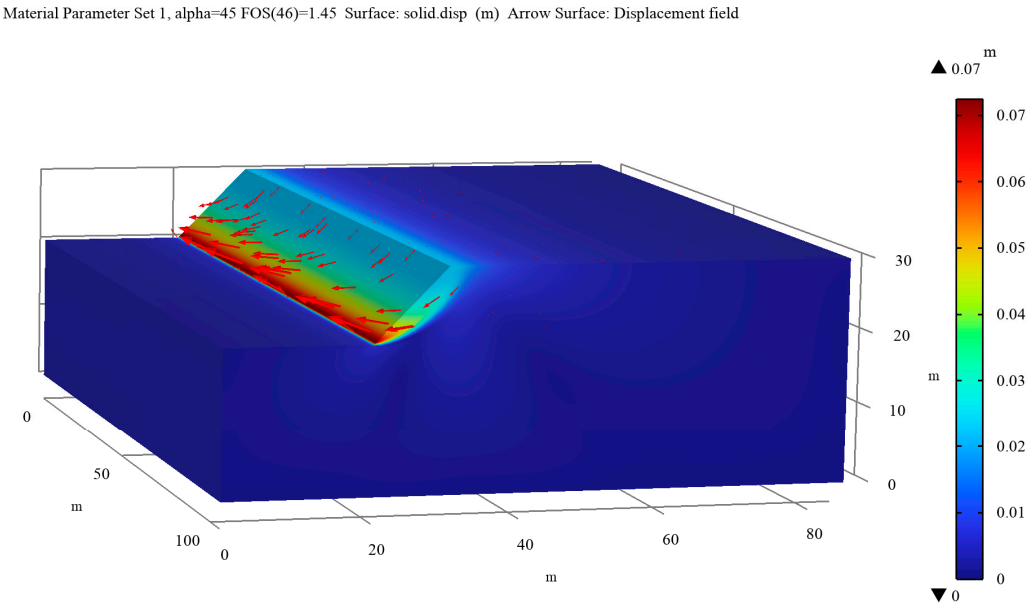

Figure 10. Displacement magnitude for a slope angle of 45°, Material 2.

Next, Figure 11 shows the 2D section displacements of the slope corresponding to Material 1, for the four slope angles considered, while Figure 12 shows the displacements for the same angles, but for Material 2.

Regarding the quantitative results, Table 4 summarizes the results obtained for all four slope angles considered and for both the non-associative flow rule and the associative flow rule.

It is observed that the FoS values corresponding to the same angle are higher for the case of the associative flow rule compared to the non-associative flow rule, which was also demonstrated by Cheng et al. [94].

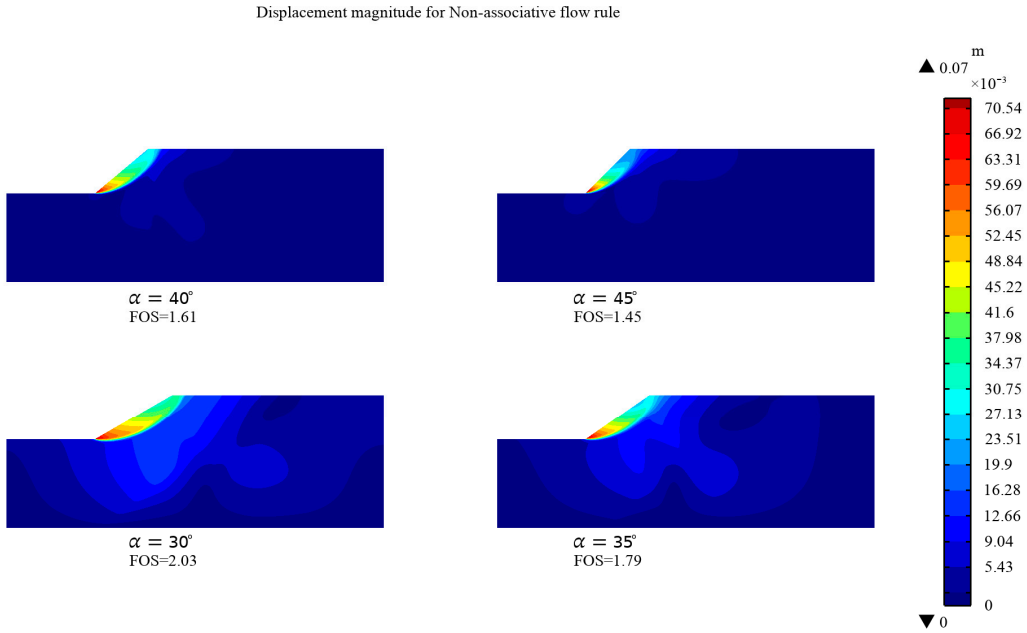

Figure 11. Slope displacements for Material 1.

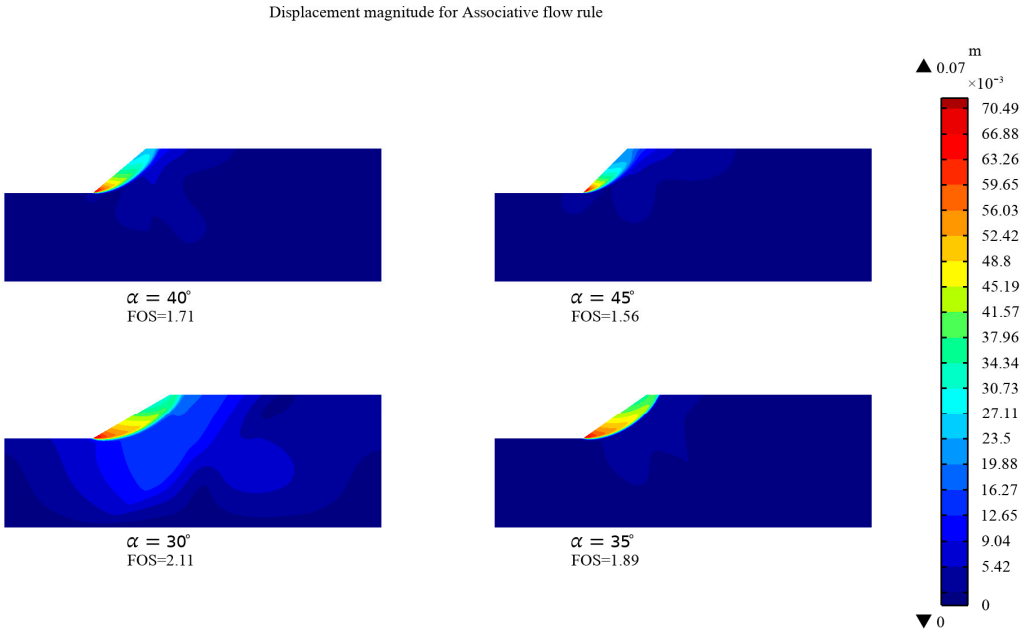

Figure 12. Slope displacements for Material 2.

Table 4. Results obtained after simulation in all scenarios.

Result	Unit	Non-Associative Flow Rule			
		A = 30°	**A = 35°**	**A = 40°**	**A = 45°**
FOS	1	2.03	1.79	1.61	1.45
Equivalent plastic strain	1	0–0.26	0–0.26	0–0.26	0–0.26
Displacement magnitude	m	0–0.072	0–0.072	0–0.072	0–0.072
		Associative flow rule			
FOS	1	2.11	1.89	1.71	1.56
Equivalent plastic strain	1	0–0.23	0–0.23	0–0.23	0–0.23
Displacement magnitude	m	0–0.072	0–0.072	0–0.072	0–0.072

The difference in FoS value increases with an increasing friction angle but the differences between the results are relatively small.

It can also be seen from Table 4 that the values corresponding to the equivalent plastic strain and the displacement magnitude do not differ between the two flow rules considered.

Also, in regard to the flow rule, the FoS and the locations of the critical failure surfaces are not greatly affected by the dilatation angle. Compared to past results employing the LEM approach [91–93], when a non-associated flow rule is assumed, the critical slip surfaces appear to be closer to those obtained using LEM than those when associated flow rule is assumed.

For both types of flow rule considered, the in situ stress due to gravity is 2.62×10^5 N/m^2. For the slope geometry considered, the maximum stress is found at the fixed base of the model. The maximum values for equivalent plastic strain and displacement magnitude correspond to the junction between the slope and the lower free part of the model.

5. Conclusions

In this study, using simulation and numerical modeling, a stability analysis was conducted for a hypothetical slope, representative in terms of its geometry, dimensions, and material characteristics of the waste dumps in the Motru coalfield in the Oltenia region of Romania. As a result of the simulations, (1) quantitative and qualitative results were obtained for the factor of safety (FoS) values for four different slope angles, in two plasticity cases. Naturally, the FoS decreases as the slope angle increases, and for the same slope angle, the FoS value for the non-associative plasticity case is always lower than that for the associative plasticity case. This indicates that the influence of considering non-associative plasticity is insignificant for the material parameter values considered. (2) The simulation results also provide an intuitive graphical representation of the equivalent plastic strain values of the studied mass for different slope angles just before the occurrence of failure (sliding), illustrating the localization of plastic strain nuclei and the failure surface for all various slope angles. This highlights the development of multiple failure surfaces within the sloped mass, a phenomenon that is more evident at smaller slope angles. (3) The 3D extension of the plane section provides a spatial representation of key characteristics like displacements, deformations, and stresses, which helps to highlight the behavior of the mass outside the sliding zone. The ability to visualize the magnitude of displacements, not just relative deformations, across the entire analyzed mass allows for a better estimation of the rock mass behavior depending on the slope angle and it also enables the correlation of qualitative aspects related to displacements and deformations with quantitative ones, such as the FoS, offering more comprehensive information for stability assessment. Moreover, the possibility of visualizing not only the magnitude of displacements but also the displacement trend—direction and orientation—at different points within the analyzed area is useful for predicting the future behavior of the slope. (4) Considering the values obtained for the FoS, it is more appropriate to use the non-associative flow rule, a conclusion also backed by [57], where Griffits et al. suggest that this flow rule should be adopted for slope stability analysis. (5) In most cases, factors like dilatation angle, soil moduli, or domain change cause differences of just a few percent and are not critical for engineering use of the SSRM.

Regarding the limitations of the SSRM generally, and when used in this research, there is a possible sensitivity to non-linear solution algorithms and flow rules in certain very special cases like soft or thin band problems, which is supported by the existing literature. Also, the method cannot detect other failure surfaces, which, even if less critical than the SSRM solution, still must be taken into consideration in engineering practice. Finally, increasing the complexity of the geometry, mesh elements, or additional variables can lead to very long computing times as compared to the LEM.

As a future research direction, we want to approach the simulation of a similar model using the FDEM technique using the Geomechanica IRAZU software and compare the results. Also, again using the COMSOL software, we want to enhance the presented model by taking into consideration the influence of water infiltration. There is a possibility to

extend the research outside of the Motru coal basin, namely to the Jilt, Rovinari, or other coal basins within the Oltenia Region, where there are dumps with different material characteristics. The model can also be adapted for the evaluation of the working face of open pit mines.

It can be concluded that the SSRM and LEM both have their respective advantages and limitations, and neither method is clearly superior for routine analysis and design. Both approaches offer only an estimation of the FoS and the likely failure mechanism, but engineers and practitioners should be mindful of the limitations of each method when conducting analyses and interpreting the results.

Author Contributions: Conceptualization, F.D.P. and A.A.; methodology, S.M.R.; software, F.D.P., A.A. and I.B.; validation, F.D.P. and C.-M.I.; writing—original draft preparation, A.A. and I.B.; writing—review and editing, F.D.P. and S.M.R. All authors have read and agreed to the published version of the manuscript.

Funding: This research received no external funding.

Institutional Review Board Statement: Not applicable.

Informed Consent Statement: Not applicable.

Data Availability Statement: Data is contained within the article. Further data on request.

Conflicts of Interest: The authors declare no conflicts of interest.

References

1. Espinoza, D.; Goycoolea, M.; Moreno, E.; Newman, A. MineLib: A library of open pit mining problems. *Ann. Oper. Res.* **2013**, *206*, 93–114. [CrossRef]
2. Wetherelt, A.; van der Wielen, K.P. Introduction to open pit mining. In *SME Mining Engineering Handbook*, 2nd ed.; Society for Mining, Metallurgy, and Exploration Inc: Englewood, CO, USA, 2011; pp. 857–875.
3. Altiti, H.; Alrawashdeh, R.; Alnawafleh, H. Open pit mining. In *Mining Techniques: Past, Present and Future*; IntechOpen: London, UK, 2021. [CrossRef]
4. Monjezi, M.; Shahriar, K.; Dehghani, H.; Samimi Namin, F. Environmental impact assessment of open pit mining in Iran. *Environ. Geol.* **2009**, *58*, 205–216. [CrossRef]
5. Zhao, Y.; Wang, Y.; Zhang, Z.; Zhou, Y.; Huang, H.; Chang, M. The Evolution of Landscape Patterns and Its Ecological Effects of Open-Pit Mining: A Case Study in the Heidaigou Mining Area, China. *Int. J. Environ. Res. Public Health* **2023**, *20*, 4394. [CrossRef] [PubMed]
6. Bell, F.G.; Donnelly, L.J. *Mining and Its Impact on the Environment*; CRC Press: London, UK, 2006. [CrossRef]
7. Dudka, S.; Adriano, D.C. Environmental impacts of metal ore mining and processing: A review. *J. Environ. Qual.* **1997**, *26*, 590–602. [CrossRef]
8. Firozjaei, M.K.; Sedighi, A.; Firozjaei, H.K.; Kiavarz, M.; Homaee, M.; Arsanjani, J.J.; Makki, M.; Naimi, B.; Alavipanah, S.K. A historical and future impact assessment of mining activities on surface biophysical characteristics change: A remote sensing-based approach. *Ecol. Indic.* **2021**, *122*, 107264. [CrossRef]
9. Tran, T.N.D.; Nguyen, Q.B.; Le, D.T.L.; Nguyen, T.D.; Vo, N.D.; Gourbesville, P. Evaluate the influence of groynes system on the hydraulic regime in the Ha Thanh River, Binh Dinh Province, Vietnam. In *Advances in Hydroinformatics: Models for Complex and Global Water Issues—Practices and Expectations*; Gourbesville, P., Caignaert, G., Eds.; Springer Water: Singapore, 2022; pp. 241–254. [CrossRef]
10. Tran, T.N.D.; Nguyen, Q.B.; Nguyen, T.T.; Vo, N.D.; Nguyen, C.P.; Gourbesville, P. Operational Methodology for the Assessment of Typhoon Waves Characteristics. Application to Ninh Thuan Province, Vietnam. In *Advances in Hydroinformatics: Models for Complex and Global Water Issues—Practices and Expectations*; Gourbesville, P., Caignaert, G., Eds.; Springer Water: Singapore, 2022; pp. 887–902. [CrossRef]
11. Saini, V.; Gupta, R.P.; Arora, M.K. Environmental impact studies in coalfields in India: A case study from Jharia coal-field. *Renew. Sustain. Energy Rev.* **2016**, *53*, 1222–1239. [CrossRef]
12. Popović, V.; Miljković, J.Ž.; Subić, J.; Jean-Vasile, A.; Adrian, N.; Nicolăescu, E. Sustainable Land Management in Mining Areas in Serbia and Romania. *Sustainability* **2015**, *7*, 11857–11877. [CrossRef]
13. Li, Z.; Ma, Z.; van der Kuijp, T.J.; Yuan, Z.; Huang, L. A review of soil heavy metal pollution from mines in China: Pollution and health risk assessment. *Sci. Total Environ.* **2014**, *468*, 843–853. [CrossRef]
14. Chaulya, S.; Prasad, G. Slope Failure Mechanism and Monitoring Techniques. In *Sensing and Monitoring Technologies for Mines and Hazardous Areas: Monitoring and Prediction Technologies*; Elsevier: Amsterdam, The Netherlands, 2016; pp. 1–86. [CrossRef]

15. Jiayin, H.; Baoan, H.; Xiangjun, T.; Jin, C.; Long, L. Concept and Practice of Open-pit Mining Area Restoration and Reuse—Taking an Open-pit Coal Mining Area in Datong, Shanxi as an Example. In *E3S Web of Conferences*; EDP Sciences: Ulys, France, 2020; Volume 145, p. 02014. [CrossRef]
16. Wang, Y.; Ni, S.-T.; Yang, F.-W.; Wang, Z.-X.; Zhang, H.; Ma, K.; Li, X.-J. Monitoring and Analysis of Dynamic Response for Open-Pit Mine with Inside Inclined Shafts under Train Loading. *Metals* **2021**, *11*, 1681. [CrossRef]
17. Blight, G.E.; Fourie, A. Catastrophe revisited–disastrous flow failures of mine and municipal solid waste. *Geotech. Geol. Eng.* **2005**, *23*, 219–248. [CrossRef]
18. Kocaman, S.; Tavus, B.; Nefeslioglu, H.A.; Karakas, G.; Gokceoglu, C. Evaluation of Floods and Landslides Triggered by a Meteorological Catastrophe (Ordu, Turkey, August 2018) Using Optical and Radar Data. *Geofluids* **2020**, *2020*, 8830661. [CrossRef]
19. Kainthola, A.; Verma, D.; Gupte, S.S.; Singh, T.N. A coal mine dump stability analysis—A case study. *Geomaterials* **2011**, *1*, 1–13. [CrossRef]
20. Behera, P.K.; Sarkar, K.; Singh, A.K.; Verma, A.K.; Singh, T.N. Dump slope stability analysis—A case study. *J. Geol. Soc. India* **2016**, *88*, 725–735. [CrossRef]
21. Kolapo, P.; Oniyide, G.O.; Said, K.O.; Lawal, A.I.; Onifade, M.; Munemo, P. An Overview of Slope Failure in Mining Operations. *Mining* **2022**, *2*, 350–384. [CrossRef]
22. Harish, P.; Chandar, K.R. A review on stability analysis of coal mine dumps. *Int. J. Min. Miner. Eng.* **2024**, *15*, 1–14. [CrossRef]
23. Yang, Z.; Ding, X.; Liu, X.; Wahab, A.; Ao, Z.; Tian, Y.; Bang, V.S.; Long, Z.; Li, G.; Ma, P. Slope Deformation Mechanisms and Stability Assessment under Varied Conditions in an Iron Mine Waste Dump. *Water* **2024**, *16*, 846. [CrossRef]
24. Xu, C.Y.; Liu, Q.S.; Tang, X.H.; Sun, L.; Deng, P.H.; Liu, H. Dynamic stability analysis of jointed rock slopes using the combined finite-discrete element method (FDEM). *Comput. Geotech.* **2023**, *160*, 105556. [CrossRef]
25. Masoudian, M.S.; Zevgolis, I.E.; Deliveris, A.V.; Marshall, A.M.; Heron, C.M.; Koukouzas, N.C. Stability and characterisation of spoil heaps in European surface lignite mines: A state-of-the-art review in light of new data. *Environ. Earth Sci.* **2019**, *78*, 505. [CrossRef]
26. Popescu, F.D.; Radu, S.M.; Andras, A.; Brinas, I.; Marita, M.-O.; Radu, M.A.; Brinas, C.L. Stability Assessment of the Dam of a Tailings Pond Using Computer Modeling—Case Study: Coroiești, Romania. *Appl. Sci.* **2024**, *14*, 268. [CrossRef]
27. Bishop, A.W. The use of the Slip Circle in the Stability Analysis of Slopes. *Géotechnique* **1955**, *5*, 7–17. [CrossRef]
28. Janbu, N. Applications of Composite Slip Surfaces for Stability Analysis. In Proceedings of the European Conference on the Stability of Earth Slopes, Stockholm, Sweden, 20–25 September 1954.
29. Morgenstern, N.; Price, V. The Analysis of the Stability of General Slip Surfaces. *Geotechnique* **1965**, *15*, 79–93. [CrossRef]
30. Spencer, E. A Method of analysis of the Stability of Embankments Assuming Parallel Inter-Slice Forces. *Géotechnique* **1967**, *17*, 11–26. [CrossRef]
31. Fredlund, D.G. Analytical methods for slope stability analysis. In Proceedings of the 4th International Symposium on Landslides, Toronto, ON, Canada, 16–21 September 1984; Volume 1, pp. 229–250.
32. Duncan, J.M. State of the art: Limit equilibrium and finite-element analysis of slopes. *J. Geotech. Eng. ASCE* **1996**, *122*, 577–596. [CrossRef]
33. Ulusay, R.; Çaglan, D.; ArIkan, F.; Yoleri, M.F. Characteristics of biplanar wedge spoil pile instabilities and methods to improve stability. *Can. Geotech. J.* **1996**, *33*, 58–79. [CrossRef]
34. Nguyen, V.U.; Nemcik, J.A.; Chowdhury, R.N. Some practical aspects of spoil pile stability by the two-wedge model. *Min. Sci. Technol.* **1984**, *2*, 57–68. [CrossRef]
35. El-Ramly, H.; Morgenstern, N.; Cruden, D. Lodalen slide: A probabilistic assessment. *Can. Geotech. J.* **2016**, *43*, 956–968. [CrossRef]
36. Husein Malkawi, A.I.; Hassan, W.F.; Abdulla, F. Uncertainty and reliability analysis applied to slope stability. *Struct. Saf.* **2000**, *22*, 161–187. [CrossRef]
37. Abdulai, M.; Sharifzadeh, M. Probability Methods for Stability Design of Open Pit Rock Slopes: An Overview. *Geosciences* **2021**, *11*, 319. [CrossRef]
38. Chuaiwate, P.; Jaritngam, S.; Panedpojaman, P.; Konkong, N. Probabilistic Analysis of Slope against Uncertain Soil Parameters. *Sustainability* **2022**, *14*, 14530. [CrossRef]
39. Chakraborty, R.; Dey, A. Probabilistic slope stability analysis: State-of-the-art review and future prospects. *Innov. Infrastruct. Solut.* **2022**, *7*, 177. [CrossRef]
40. Antolini, F.; Barla, M.; Gigli, G.; Giorgetti, A.; Intrieri, E.; Casagli, N. Combined finite–discrete numerical modeling of runout of the Torgiovannetto di Assisi rockslide in central Italy. *Int. J. Geomech.* **2016**, *16*, 04016019. [CrossRef]
41. Koner, R.; Chakravarty, D. Numerical analysis of rainfall effects in external overburden dump. *Int. J. Min. Sci. Technol.* **2016**, *26*, 825–831. [CrossRef]
42. Yang, Y.; Hong, Z. Direct Approach to Treatment of Contact in Numerical Manifold Method. *Int. J. Geomech.* **2017**, *17*, e4016012. [CrossRef]
43. Nguyen, P.M.V.; Wrana, A.; Rajwa, S.; Różański, Z.; Frączek, R. Slope Stability Numerical Analysis and Landslide Prevention of Coal Mine Waste Dump under the Impact of Rainfall—A Case Study of Janina Mine, Poland. *Energies* **2022**, *15*, 8311. [CrossRef]
44. Guanhua, Q. Stability analysis of nonhomogeneous and anisotropic stepped slopes under the influence of earthquakes. *Heliyon* **2023**, *9*, e15057. [CrossRef]

45. Sun, L.; Liu, Q.; Abdelaziz, A.; Tang, X.; Grasselli, G. Simulating the entire progressive failure process of rock slopes using the combined finite-discrete element method. *Comput. Geotech.* **2022**, *141*, 104557. [CrossRef]
46. Rudra, E.S.C.K.; Gadepaka, P.R.; Rai, R.; Jaiswal, A. Numerical analysis of dump slope stability using material properties obtained by parallel gradation method. *Min. Technol. Trans. Inst. Min. Metall.* **2024**, *133*, 31–41. [CrossRef]
47. Xu, H.; He, X.; Shan, F.; Niu, G.; Sheng, D. Machine Learning in the Stochastic Analysis of Slope Stability: A State-of-the-Art Review. *Modelling* **2023**, *4*, 426–453. [CrossRef]
48. Mahmoodzadeh, A.; Alanazi, A.; Hussein Mohammed, A.; Hashim Ibrahim, H.; Alqahtani, A.; Alsubai, S.; Babeker Elhag, A. Comprehensive analysis of multiple machine learning techniques for rock slope failure prediction. *J. Rock Mech. Geotech. Eng.* 2023, *in press*. [CrossRef]
49. Meng, J.; Mattsson, H.; Laue, J. Three-dimensional Slope Stability Predictions Using Artificial Neural Networks. *Int. J. Numer. Anal. Methods Geomech.* **2021**, *45*, 1988–2000. [CrossRef]
50. Ji, J.; Zhang, C.; Gui, Y.; Lü, Q.; Kodikara, J. New Observations on the Application of LS-SVM in Slope System Reliability Analysis. *J. Comput. Civ. Eng.* **2017**, *31*, 06016002. [CrossRef]
51. Falae, P.O.; Agarwal, E.; Pain, A.; Dash, R.K.; Kanungo, D.P. A Data Driven Efficient Framework for the Probabilistic Slope Stability Analysis of Pakhi Landslide, Garhwal Himalaya. *J. Earth Syst. Sci.* **2021**, *130*, 167. [CrossRef]
52. Cundall, P.A. A computer model for simulating progressive, large-scale movements in blocky rock systems. In Proceedings of the International Symposium on Rock Mechanics, Nancy, France, 4–6 October 1971; Volume 1, pp. 8–11.
53. Regassa, B.; Xu, N.; Mei, G. An equivalent discontinuous modeling method of jointed rock masses for dem simulation of mining-induced rock movements. *Int. J. Rock Mech. Min. Sci.* **2018**, *108*, 1–14. [CrossRef]
54. Zhao, J.; Zhu, Z.; Zhang, D.; Wang, H.; Li, X. Assessment of Fabric Characteristics with the Development of Sand Liquefaction in Cyclic Triaxial Tests: A DEM Study. *Soil Dyn. Earthq. Eng.* **2024**, *176*, 108343. [CrossRef]
55. Wang, H.; Zhang, B.; Mei, G.; Xu, N. A statistics-based discrete element modeling method coupled with the strength reduction method for the stability analysis of jointed rock slopes. *Eng. Geol.* **2020**, *264*, 105247. [CrossRef]
56. Gupta, G.; Sharma, S.K.; Singh, G.S.P.; Kishore, N. Numerical Modelling-Based Stability Analysis of Waste Dump Slope Structures in Open-Pit Mines—A Review. *J. Inst. Eng. India Ser. D* **2021**, *102*, 589–601. [CrossRef]
57. Griffiths, D.V.; Lane, P.A. Slope stability analysis by finite elements. *Geotechnique* **1999**, *49*, 387–403. [CrossRef]
58. Dyson, A.P.; Tolooiyan, A. Optimisation of strength reduction finite element method codes for slope stability analysis. *Innov. Infrastruct. Solut.* **2018**, *3*, 38. [CrossRef]
59. Sun, G.; Lin, S.; Zheng, H.; Tan, Y.; Sui, T. The virtual element method strength reduction technique for the stability analysis of stony soil slopes. *Comput. Geotech.* **2020**, *119*, 103349. [CrossRef]
60. Zienkiewicz, O.C.; Humpheson, C.; Lewis, R.W. Associated and non-associated visco-plasticity and plasticity in soil mechanics. *Geotechnique* **1975**, *25*, 671–689. [CrossRef]
61. Griffiths, D.V. Finite Element Analyses of Walls, Footings and Slopes. Ph.D. Thesis, Univ. of Manchester, Manchester, UK, 1981.
62. Naylor, D.J. Finite Elements and Slope Stability. In *Numerical Methods in Geomechanics. NATO Advanced Study Institutes Series*; Martins, J.B., Ed.; Springer: Dordrecht, Germany, 1982; Volume 92, pp. 229–244. [CrossRef]
63. Smith, I.M.; Griffiths, D.V. *Programming the Finite Element Method*; John Wiley & Sons, Inc.: Hoboken, NJ, USA, 1988.
64. Matsui, T.; San, K.-C. Finite Element Slope Stability Analysis by Shear Strength Reduction Technique. *Soils Found.* **1992**, *32*, 59–70. [CrossRef]
65. Zhu, H.; Wang, Z.; Shi, B.; Wong, J.K. Feasibility study of strain based stability evaluation of locally loaded slopes: Insights from physical and numerical modeling. *Eng. Geol.* **2016**, *208*, 39–50. [CrossRef]
66. Zou, P.; Zhao, X.; Meng, Z.; Li, A.; Liu, Z.; Hu, W. Sample Rocks Tests and Slope Stability Analysis of a Mine Waste Dump. *Adv. Civ. Eng.* **2018**, *2018*, 6835709. [CrossRef]
67. Meng, W.; Wang, H.; Cai, M.; Zhang, Q. Multi. scale strength reduction method for heterogeneous slope using hierarchical FEM/DEM modeling. *Comput. Geotech.* **2019**, *115*, 103164. [CrossRef]
68. Yang, Y.; Sun, G.; Zheng, H. Stability analysis of soil-rock-mixture slopes using the numerical manifold method. *Eng. Anal. Bound. Elem.* **2019**, *109*, 153–160. [CrossRef]
69. Yang, Y.; Sun, G.; Zheng, H.; Yan, C. An improved numerical manifold method with multiple layers of mathematical cover systems for the stability analysis of soil-rock-mixture slopes. *Eng. Geol.* **2020**, *264*, 105373. [CrossRef]
70. Dyson, A.P.; Griffiths, D.V. An Efficient Strength Reduction Method for Finite Element Slope Stability Analysis. *Comput. Geotech.* **2024**, *174*, 106593. [CrossRef]
71. Itasca. *FLAC Version 7.0 User's Manual*; Itasca Consulting Group, Inc: Minneapolis, MN, USA, 2011.
72. Itasca. *3DEC 9.0 User's Manual*; Itasca Consulting Group, Inc: Minneapolis, MN, USA, 2011.
73. Brinkgreve, R.B.J.; Engin, E.; Swolfs, W.M. *PLAXIS 3D 2013 User Manual*; Plaxis BV: Delft, The Netherlands, 2013.
74. Tran, T.N.D.; Ahmed, Z.; Nguyen, Q.B. Application of Plaxis for calculating the construction stability and soft embankment in protecting Ha Thanh river, Binh Dinh Province. In Proceedings of the 2nd Conference on Sustainability in Civil Engineering (CSCE'20), Department of Civil Engineering Capital University of Science and Technology, Islamabad, Pakistan, 12 August 2020; pp. 418–425.
75. Rocscience. *Phase2 v6.0—A Two-Dimensional Finite Element Analysis Program*; ROCSCIENCE Inc: Toronto, ON, Canada, 2005.
76. Rocscience. *Slide v5.0—A Slope Stability Program Based on Limit-Equilibrium Analysis*; ROCSCIENCE Inc: Toronto, ON, Canada, 2003.

77. COMSOL. *COMSOL Multiphysics 5.3. Reference Manual*; COMSOL AB: Stockholm, Sweden, 2017.
78. Wu, D.; Deng, T.; Duan, W.; Zhang, W. A coupled thermal-hydraulic-mechanical application for assessment of slope stability. *Soils Found.* **2019**, *59*, 2220–2237. [CrossRef]
79. Shao, W.; Bogaard, T.; Bakker, M. How to use COMSOL multiphysics for coupled dual-permeability hydrological and slope stability modeling. *Procedia Earth Planet. Sci.* **2014**, *9*, 83–90. [CrossRef]
80. Sysala, S.; Tschuchnigg, F.; Hrubesova, E.; Michalec, Z. Optimization variant of the shear strength reduction method and its usage for stability of embankments with unconfined seepage. *Comput. Struct.* **2023**, *281*, 107033. [CrossRef]
81. Sysala, S.; Hrubešová, E.; Michalec, Z.; Tschuchnigg, F. A Rigorous Variant of the Shear Strength Reduction Method and Its Usage in Slope Stability. In *Challenges and Innovations in Geomechanics. IACMAG 2022. Lecture Notes in Civil Engineering*; Barla, M., Di Donna, A., Sterpi, D., Insana, A., Eds.; Springer: Cham, Switzerland, 2022; Volume 288. [CrossRef]
82. Zhang, C.; Duan, P.; Cheng, Y.; Chen, N.; Huang, H.; Xiong, F.; Dong, S. A 2-D stability analysis of surrounding rock of underground liquified natural gas storage cavern based on COMSOL Multiphysics. *Energy Geosci.* **2024**, *5*, 100301. [CrossRef]
83. Popescu, F.D.; Radu, S.M.; Andraș, A.; Brînaș, I.; Budilică, D.I.; Popescu, V. Comparative Analysis of Mine Shaft Hoisting Systems' Brake Temperature Using Finite Element Analysis (FEA). *Materials* **2022**, *15*, 3363. [CrossRef] [PubMed]
84. Andras, A.; Brînas, I.; Radu, S.M.; Popescu, F.D.; Popescu, V.; Budilica, D.I. Investigation of the Thermal Behaviour for the Disc-Pad Assembly of a Mine Hoist Brake Using COMSOL Multiphysics. *Acta Tech. Napoc. Ser. Appl. Math. Mech. Eng.* **2021**, *64*, 227–234.
85. Oberhollenzer, S.; Tschuchnigg, F.; Schweiger, H.F. Finite element analysis of slope stability problems using non-associated plasticity. *J. Rock Mech. Geotech. Eng.* **2018**, *10*, 1091–1101. [CrossRef]
86. Schweiger, H.F.; Tschuchnigg, F. Strength reduction technique with finite element method for slopes without stabilisation measures. *Ground Eng.* **2022**, *1*, 27–34.
87. Davis, E.H. Theories of plasticity and failure of soil masses. In *Soil Mechanics: Selected Topics*; Lee, I.K., Ed.; Elsevier: New York, NY, USA, 1968.
88. *U.M.C. Lupoaia, Oltenia Energy Complex 2021–2023*; Oltenia Energy Complex: Târgu Jiu, Romania, Internal Report; nonpublic document. (In Romanian)
89. *U.M.C. Roșiuța, Oltenia Energy Complex 2020–2022*; Oltenia Energy Complex: Târgu Jiu, Romania, Internal Report; nonpublic document. (In Romanian)
90. Geologic Lab Ltd. *Test Reports No. 014533/from 23.11.2021*; Geologic Lab Ltd.: Călan, Romania, 2021.
91. Lazăr, M.; Faur, F. *Stability and Arrangement of Slopes. Examples of Calculation*; Universitas: Petrosani, Romania, 2015; ISBN 978-973-741-453-3. (In Romanian)
92. Lazar, M.; Faur, F.; Apostu, I.-M. Stability Conditions in Lignite Open Pits from Romania, Case Study: Olteț u Open Pit. *Appl. Sci.* **2022**, *12*, 9607. [CrossRef]
93. Faur, F.; Apostu, I.-M.; Lazăr, M. Reassessment of the Stability Conditions in the Lignite Open Pits of Oltenia (Romania) in Relation to the New Local Seismic Context as an Imperative for Sustainable Mining. *Sustainability* **2024**, *16*, 1384. [CrossRef]
94. Cheng, Y.M.; Lansivaara, T.; Wei, W.B. Two-dimensional slope stability analysis by limit equilibrium and strength reduction methods. *Comput. Geotech.* **2007**, *34*, 137–150. [CrossRef]